AD-A082 381 SYRACUSE UNIV NY F/G 17/8
GEOMETRY OF ORBITING EARTH SATELLITES (GOES).(U)
JAN 80 J L POSDAMER F30602-75-C-0121
UNCLASSIFIED RADC -TR-79-357 NL

END
DATE FILMED
4-80
DTIC

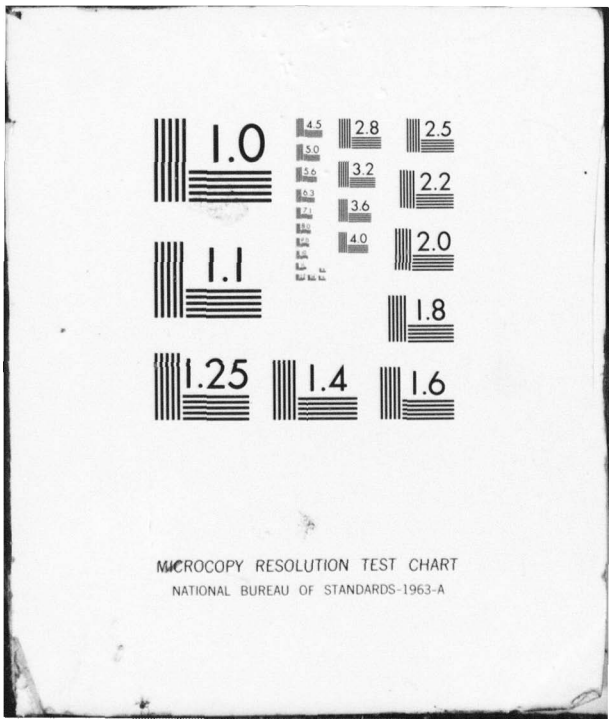
1.0
1.1
1.25
1.4
1.6
1.8
2.0
2.2
2.5
2.8
3.2
3.6
4.0
4.5
5.0
5.6
6.3
7.1
MICROCOPY RESOLUTION TEST CHART
NATIONAL BUREAU OF STANDARDS-1963-A

(12) LEVEL II

RADC-TR-79-357
Final Technical Report
January 1980

GEOMETRY OF ORBITING EARTH SATELLITES (GOES)

Syracuse University

Jeffrey L. Posdamer

Laboratory Directors' Fund 017278P1

ROME AIR DEVELOPMENT CENTER
Air Force Systems Command
Griffiss Air Force Base, New York 13441

This report has been reviewed by the RADC Public Affairs Office (PA) and is releasable to the National Technical Information Service (NTIS). At NTIS it will be releasable to the general public, including foreign nations.

RADC-TR-79-357 has been reviewed and is approved for publication.

APPROVED:

DELBERT G. KULCHAK
Project Engineer

APPROVED:

OWEN R. LAWTER, Colonel, USAF
Chief, Intelligence and Reconnaissance Division

FOR THE COMMANDER:

JOHN P. HUSS
Acting Chief, Plans Office

If your address has changed or if you wish to be removed from the RADC mailing list, or if the addressee is no longer employed by your organization, please notify RADC (IRD), Griffiss AFB NY 13441. This will assist us in maintaining a current mailing list.

Do not return this copy. Retain or destroy.

UNCLASSIFIED

SECURITY CLASSIFICATION OF THIS PAGE *(When Data Entered)*

REPORT DOCUMENTATION PAGE

READ INSTRUCTIONS BEFORE COMPLETING FORM

1. REPORT NUMBER: RADC-TR-79-357	2. GOVT ACCESSION NO.
3. RECIPIENT'S CATALOG NUMBER	
4. TITLE *(and Subtitle)*: GEOMETRY OF ORBITING EARTH SATELLITES (GOES)	5. TYPE OF REPORT & PERIOD COVERED: Final Technical Report. January 1978 — July 1979
	6. PERFORMING ORG. REPORT NUMBER: N/A
7. AUTHOR(s): Dr. Jeffrey L. Posdamer*	8. CONTRACT OR GRANT NUMBER(s): F30602-75-C-0121
9. PERFORMING ORGANIZATION NAME AND ADDRESS: Syracuse University, Syracuse NY 13210	10. PROGRAM ELEMENT, PROJECT, TASK AREA & WORK UNIT NUMBERS: 61101F, 017278P1
11. CONTROLLING OFFICE NAME AND ADDRESS: Rome Air Development Center (IRD), Griffiss AFB NY 13441	12. REPORT DATE: January 1980 13. NUMBER OF PAGES: 60
14. MONITORING AGENCY NAME & ADDRESS *(if different from Controlling Office)*: Same	15. SECURITY CLASS. *(of this report)*: UNCLASSIFIED 15a. DECLASSIFICATION/DOWNGRADING SCHEDULE: N/A

16. DISTRIBUTION STATEMENT *(of this Report)*

Approved for public release; distribution unlimited

17. DISTRIBUTION STATEMENT *(of the abstract entered in Block 20, if different from Report)*

Same

18. SUPPLEMENTARY NOTES

*SUNY at Buffalo, Buffalo NY

RADC Project Engineer: Delbert G. Kulchak, Major, USAF (IRD)
This effort was funded in whole by the RADC Laboratory Directors' Fund 017278P1.

19. KEY WORDS *(Continue on reverse side if necessary and identify by block number)*

Pattern Recognition
Satellite Identification
Signal Processing
Specular Detection

20. ABSTRACT *(Continue on reverse side if necessary and identify by block number)*

This report describes the results of a study undertaken to determine if apparent satellite brightness as measured at earth tracking stations could be used to determine the geometry of the specular reflectors on the orbiting earth satellite. Specular peaks were identified in the data, sequences of peaks were traced, the maximum peak was identified, and the area and orientation of the maximum peaks were calculated. The output of the specular detection process can be interactively edited to allow translation and rotation of the polygons

(over)

DD FORM 1 JAN 73 1473 EDITION OF 1 NOV 65 IS OBSOLETE

UNLCASSIFIED

SECURITY CLASSIFICATION OF THIS PAGE *(When Data Entered)*

339600

JOB

generated. The process cannot provide unique solutions to the reconstruction problem without some prior knowledge of the object's surface geometry, however. While the feasibility of this approach has been demonstrated, additional work in the areas of simulation, signal processing, and pattern recognition is required.

Abstract

A study was undertaken to determine if apparent satellite brightness as measured at earth tracking stations could be used to determine the geometry of the specular reflectors on an orbiting earth satellite. It has been determined that by use of appropriate processing techniques including interactive graphic editing, this task could be accomplished. More importantly, the study concludes that the determination of a geometry which is equivalent in reflective behavior to the satellite (an albedomorph) could be determined from the given data.

After development of an appropriate mathematical model, techniques for solution of the resulting system of equations are suggested. The development of a phantom generation system for solution verification is discussed. Development of a data base for measurement data is analyzed. Use of signal processing to condition the noisy and intermittent data is proposed. The use of pattern recognition techniques for identification of and compensation for standard satellite components is suggested.

Table of Contents

EVALUATION

This study was undertaken to determine the feasibility of reconstructing composite images of distant space objects from photometric signature data. The study consisted of basic research directed toward the development of an interactively edited system which could display representations of the area and orientation of specular reflectors on the surface of the space object. The significance of this effort lies in the unique fashion in which space objects may be identified, in near-real time, with existing photometric data gathering systems. The results may have applications in a host of Indications and Warning functions performed throughout the intelligence community.

DELBERT G. KULCHAK, Major, USAF
Project Engineer

1. Introduction

Few people of a scientific mind have not observed an orbitting earth satellite as it crosses the early evening or pre-morning sky. A combination of such elements as the observer's position, the satellite's orbit and the sun's position create the environment for such an observation. While it may not be apparent to the earth bound observer, the perceived brightness of the point in the sky which is the satellite varies on an instantaneous basis. Observational factors including atmospheric interference and sky light variations account for some of this. A substantial portion of the variation in brightness is attributable to the variations in light reflected from the surface of the satellite as it rotates about its central axis for stability.

The problem to be examined is: Can the surface geometry of an orbiting satellite be determined from the brightness data? This provides a passive means of satellite identification which requires no transmission of energy which can be perceived by the satellite.

2. Mathematical Models

Before attempting to analyze a problem such as this, it is necessary to develop a mathematical model of the physical phenomenon. An examination of the available open* literature provides little information dealing directly with the problem at hand. A substantial literature exists for some related topics. The synthesis of realistic properties has been presented by Phong (1), Catmull (2), Gouraud (3), Greenberg (4) and many others. The second category of research is that specifically dealing with determination of an object's shape from shading information. Work by Horn (5) is the most relevant to this topic. Last, as will become apparent, the determination of shape from a series of brightness measurements can be treated as the determination of a set of values from a series of projections (brightness measurements) of those values. A substantial body of work which addresses the value-from-projections problem is associated with computer-assisted-tomography (6) and related problems in electron microscopy (7), lunar (8) and solar (9) astronomy.

An examination of single reflectors will be followed by development of techniques appropriate for multiple reflector systems.

---

* The author has had no access to any restricted literature dealing with this research.

2.1 Single planar reflectors

While it is clear from photographs of existing satellites that portions of their structures are constructed from units using continuous elements such as cones, parabaloids or spheres, the geometric model to be used here is that of a collection of planar polygons. The reasons for this choice include computational manageability and appropriateness to available solution techniques.

While computational approaches to continuous surface modelling have been attempted, notably by Horn, they are inappropriate to this problem. A satellite typically has significant portions of its surface fabricated from planar components, e.g. panels, solar cells, etc. The available solution techniques including graphic editing and the proposed techniques to attack the albedomorph problem are oriented to discrete planar components. Since the satellite's geometry is to be modelled as a collection of planar polygons, it will be useful to begin by examining the properties of single reflectors. The discussion will follow the notation of Horn (10).

Consider the (pseudo-) planar segment of a reflecting surface as shown in Figure 2.1. With respect to this surface, there are three relevant angles for discussion of reflection computation. Consider the vector $\bar{N}_p$ to be an outward pointing surface normal at a point (P) on the surface. The angle i denotes the angle between $\bar{N}_p$ and a vector pointing

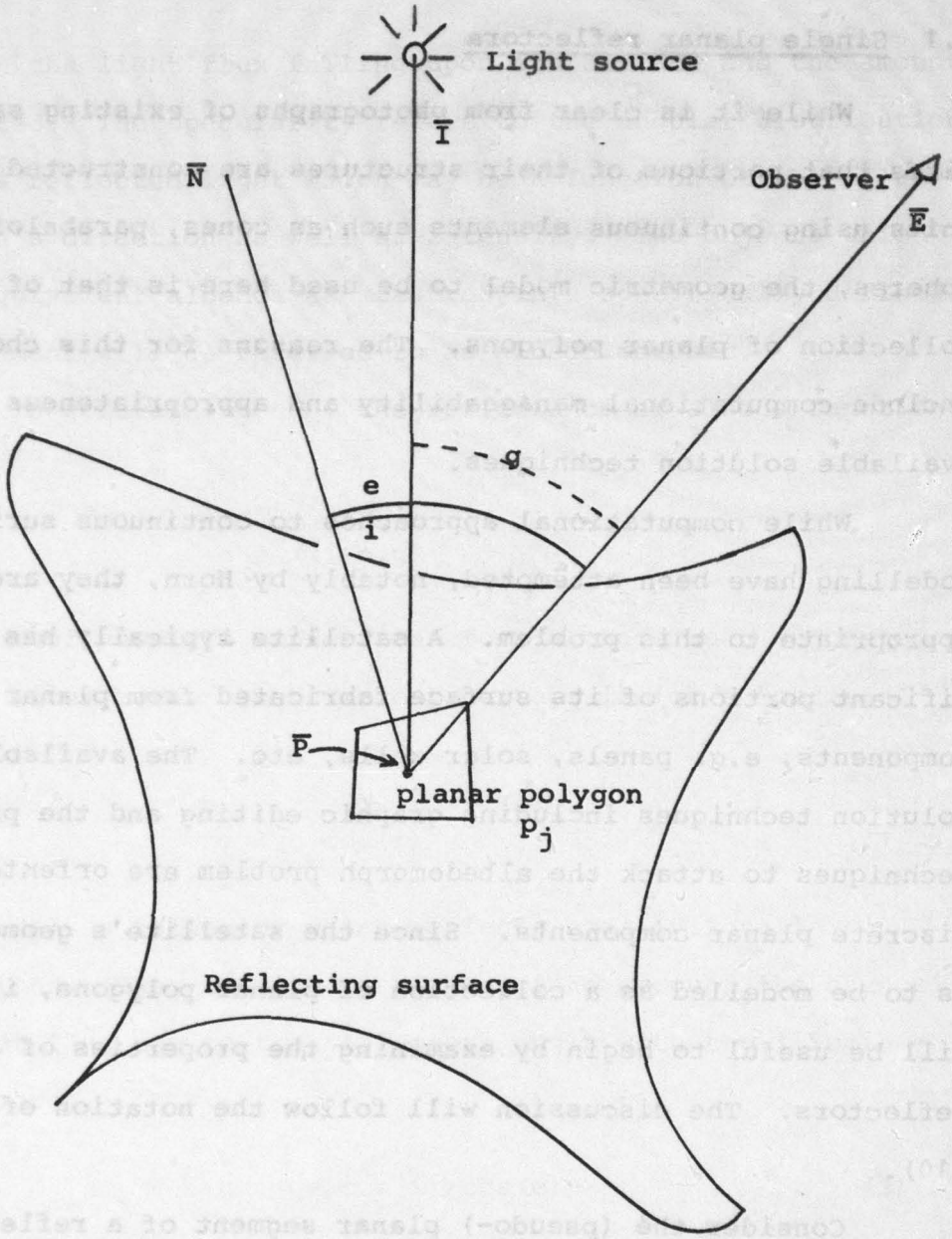

Fig. 2.1 Planar polygonal portion of reflecting surface

to the illumination source. The angle e specifies a similar angular measure (the emittance angle) between the normal and the observer. Lastly, the angle g denotes the angle between illuminator and observer. It is worth noting that in the case of an orbiting satellite the distances to the illuminator and the observer are so large as to be reasonably considered to be infinite.

The amount of light energy received by an observer from the reflector is a function of several factors. These include the incident illumination, the reflective properties of the surface, the transmission properties and the signal measurement process.

Because the illuminator in this case is the sun, it is reasonable to assume uniform incident light flux over the polygon. It is important to note at this point that the sun is not a point light source but one of finite angular dimension (approximately $.5^{o}$). There are significant factors introduced into the data by atmospheric turbulance and turbidity as well as measurement error. For present purposes, these effects will not be analyzed.

For the problem at hand, discussion will be restricted to a simple mathematical model of reflection similar to those used in visual simulation and scene synthesis. Two particular properties of the reflector, reflectance and specularity, are significant and interrelated. The term albedo (α) will be used (perhaps too generally) for the combination of these two properties. The reflectance (ρ) of a surface is the ratio

between the light flux falling upon its surface and the amount reflected. The specularity refers to the angular distribution of this reflected light which may be a function of the illumination's direction as well as intensity. Two objects which have equivalent albedos as measured in a specifically defined environment will be referred to as albedo-morphic.

In general let α, the reflectance or albedo function be:

$$\alpha \equiv f(i,e,g)$$

A number of possible expressions for α have been suggested on the literature. The simplest perhaps is for a "perfect" diffuser:

$$\alpha \equiv \rho \cos(i) \qquad (1)$$

This models a reflector which reflects equally in all directions. The $\cos(i)$ term takes into account the change in input flux due to the reflectors angle with the illumination source.

$$\alpha_R = \rho \cos(i)/\cos(e) \qquad (2)$$

is suggested for rocky terrain and/or soil. A more elaborate function has been suggested (10) for the general problem

$$\alpha_y = \rho_1 \cos(e)\cos(i) + \rho_2 (\cos(i))^n \qquad (3)$$

where the first term corresponds to diffuse reflection and the second the more highly directional specular. A simplification of α_y which is useful is

$$\alpha_G = (\cos(e)\cos(i))^n \qquad (4)$$

in which n is varied as a measure of specularity. This simplification results from treating the surface as a combination diffuse/specular reflector which may be characterized with a single "compromise" albedo. Since each of the functions is a point wise reflection function, b_j (the total light reflected by a surface (j)) will be noted as

$$b_j = a_j \alpha_j \quad \text{where } a \text{ is the area.} \qquad (5)$$

2.2 Coordinate systems

At least three significant coordinate systems exist in the description of this problem. These are the observers' azimuth-elevation system; the observers' astronomical system; and the satellite local system. Three significant objects exist: (1) the observer; (2) the sun; and, (3) the satellite. In choosing a system, it is clear that the relative motion of the observer, sun and satellite must be described. The satellite, it should be noted, is considered to rotate about its own axis. The axis of rotation is considered to be normal to the earth's surface.

After consideration, a satellite local coordinate system was chosen. Since the satellite is the object of interest, a satellite local system simplifies definition of the geometry. In reality, two linked satellite local systems are used and expressed in spherical coordinates. The satellite

geometry is modelled as a set of planar polygons, whose normals are expressed in terms of ϕ_σ, θ_σ , the coordinate system fixed to the satellite "physical" structure itself. That is, ϕ_σ and θ_σ do not change as the satellite rotates. A second local system, a "box" in which the satellite rotates, is rated ϕ_Σ , θ_Σ . For a given spherical coordinate $\phi_\Sigma = \phi_\sigma$. For a satellite rotational period of τ ,

$$\theta_\sigma = 2\pi\left(\frac{t \text{ MOD } \tau}{\tau}\right) + \theta_\Sigma \qquad (6)$$

Obviously, it is necessary to define i, e and g now in terms of $[{}_i\phi_\Sigma(t), {}_i\theta_\Sigma(t)]$, $[{}_e\theta_\Sigma(t), {}_e\theta_\Sigma(t)]$ and $[{}_g\phi_\Sigma(t), {}_g\theta_\Sigma(t)]$. The normal of polygon j will be denoted as $[{}_j\phi_\Sigma(t), {}_j\theta_\Sigma(t)]$ or $[{}_j\phi_\sigma, {}_j\theta_\sigma]$.

2.3 Collections of reflectors

As noted earlier, the model to be used for this system is that of a collection of planar reflectors approximating the surface of the satellite. Because of the distances involved, the only measurement available is the total reflected light from the surface of the satellite. This may be viewed as the integral (or sum) of the brightness values over an image of the satellite if such an image could be obtained. Since a discrete model is being used, the summation over N polygons is appropriate. Thus at time t, B(t) , the total measured brightness is

$$B(t) = \sum_{j=1}^{N} b_j(t) = \sum_{j=1}^{N} a_j \alpha_j(t) \qquad (7)$$

where α varies with time due to the variation of i, e and g with time. The total brightness is the sum of the contributions of the individual surface components. As noted in equations 1-4, the reflected flux, as a function of i, e and/or g , will vary over time.

No mention has been made until now of problems associated with hidden surfaces, visual priority and shadowing, the last of these being merely a variation of the first two. The term interference will be used to group these problems under a single heading. Two aspects of interference are significant. For any single polygon, self-interference is the situation when the polygon's "body" lies between its surface and the significant entity (sun or observer). A more difficult problem arises when a second polygon interferes with the first (obscuration).

Self-interference (intraference (?)) is easily resolved. In visual simulation, the solution is referred to a rear-face cull. In the context of the satellite geometry problem, the solution is likewise simple. If $-\pi/2 \leq i(t) \leq \pi/2$, then the polygon faces away from the sun (because angle of incidence exceeds 90°) and cannot be illuminated and thus makes no contribution to B(t) . For $-\pi/2 \leq e(t) \leq \pi/2$, the polygon cannot be seen (that is, only the "back" of the polygon faces the observer) and similarly makes no contribution to B(t) .

The problem of obscuration is considerably more difficult to deal with. If a polygon is obscured with respect to the sun then its contribution to B(t) is diminished because it is in shadow. If it is obscured with respect to the observer, then its contribution is diminished because the light it reflects never reaches the observer. For a predetermined geometry, a vast array of techniques exist for calculating obscuration. Unfortunately, the problem to be solved is to determine an unknown geometry. The effect of obscuration, then, is to create a polygon whose area seems to vary over time. If such pseudo-time-varying (PTV) polygons can be detected, they could be used to provide significant geometric information.

The problem of non-uniqueness is another serious issue when dealing with collections of polygons. For each instantaneous brightness measurement, an equation of the form used in equation (7) will be created. This specifically results from choosing a form for $\alpha(i,e,g)$ and a priori knowledge of the relative angular positions of reflecting object, source and observer. Examination of the form of this system of non-linear equations yields reflectivity, area and specularity of the individual surface elements as the unknowns. Obviously, assuming fixed values for any of these variables leads to solution of the others. If two polygons are parallel, there appears no means of solving the equation to yield two or more areas for a given orientation. Unless additional properties are derivable from other aspects of data analysis (e.g.

obscuration detection), solutions for multiple parallel reflectors will not be unique.

A similar problem of ambiguity exists. The area of a reflector may be determined by solution of a system of equations resulting from (7). No means is provided to determine shape, however. A similar ambiguity exists with respect to the position of the reflector. The albedo for each reflector defined by its orientation may be determined from solution of the equations. However, this does not provide data concerning the position of the given reflector.

It is clear from the preceding comments that a unique, unambiguous solution to the geometry problem cannot be obtained from a system of equations derived from (7). A solution of such a set of equations can be obtained which are albedomorphic with the actual satellite. With the addition of non-algebraic processing and heuristic constraints, it appears that the albedomorphic could be improved. The use of pattern recognition techniques will be discussed in Section 2.5. It seems at this point, however, that a unique, non-ambiguous solution to the problem is not possible. The quality of an albedomorphic solution is unknown and requires considerable future research.

2.4 Surface geometry as a projection problem

It will be useful now to restate the orbiting satellite surface geometry problem.

An object is in orbit about the earth. At times it is illuminated by the sun and simultaneously observed from the earth's surface. Measurements are taken of the light it reflects. From these measurements (and minimal a priori data), create an approximation of the object's surface geometry.

In light of the discussions of the earlier sections, let us examine the problem. A model of the surface has been chosen. It consists of a surface tesselation of a sphere with a finite set of planar polygons $p_j \leq \{P\}$ whose surface normals are uniformly distributed in spherical coordinates such that, if they were equal in area, they would approximate a spherical surface. The spheres' orientation with respect to illumination and the observer vary over time in a deterministic manner (the a priori data allows for calculation of illumination/observer position). A subset $\{I\} \subset \{P\}$ (approximately half) of the surface model polygons are not self-shadowed, i.e. are illuminated. A subset $\{V\} \subset \{P\}$ of the surface polygons are visible to the observer. At any point in time (t), $I \cap V$ contribute non-zero elements to the summation $B(t)$. The brightness is measured at a large number of points in time.

Using equations 4, 5 and 7 we now get:

$$B(t) = \sum_{j=1}^{N} a_j \rho_j (\cos(e(t))\ \cos(i(t)))^{n_j} \qquad (8)$$

for j such that $\rho_j \subseteq (I \cap V)$

Given this set of equations, solve for

a) a_j, ρ_j, n_j

b) a_j, ρ_j assuming values for n_j (assuming specularity constant)

c) a_j assuming values for ρ_j, n_j (assuming albedo constant)

Note that c) is a linear set of equations. Also note that in the data provided, the number of measurements greatly exceeds N.

The problem, thus translated, seems still to be excessively large given reasonable resolutions, i.e., several hundred values of N. Once more, briefly restating the problem:

> Given a set of N unknowns, a series of weighted sums of those unknowns in which the individual sets of non-zero weights are much less than the total unknowns, and, lastly, a set of geometric constraints, approximate a reasonable set of values for the unknowns in a computationally efficient manner.

A similar problem abstraction exists for a class of problems jointly known as reconstruction from projection problems. Problems of this class are characterized by the

presentation of a set of measurements of a physically significant quantity. In the case of computerized axial tomography (CAT), these consist of X-ray measurements from a variety of orientations around the region of interest. Typically, an X-ray source is moved in a planar path around a "slice" of the body and the transmitted rays measured after passage through the target. Each individual measurement thus represents the effects of the absorption coefficient of the total material in the path through which the individual ray has passed. A useful mathematical model for the slice under examination is a regular rectangular grid of absorption elements. The problem, then, is to approximate the absorption or density values over the grid from a set of measurements. Each ray measurement is thus taken to be the sum of the effects of the density elements intersected by the ray. Each ray measurement is then taken to be directly related to a projection of the attenuation elements which it intersects. A substantial array of mathematical and computational tools exist for solution of this class of problems.

It is a basic contention of this research that the determination of an albedomorphic object from brightness measurements is, in its essential mathematical and computational aspects, a problem in reconstruction from projections.

2.5 Pattern recognition

The problems of ambiguity and non-uniqueness, as defined above, will not permit an analysis at this point of

the relationship between albedomorphic geometry and actual satellite geometry. Even when an albedomorphic solution has been obtained, it is clear that there are severe problems inherent in the mathematical model which will prohibit the creation of unique, unambiguous solutions. The underlying reason for these problems is the generality of the mathematical model. It assumes no a priori knowledge of satellite surface geometry. The use of the existing a priori knowledge of satellite surface geometry will be as a basis for pattern recognition techniques applied to the measured data.

The specific study discussed in the latter part of this document, the specular reflector geometry, represents an example of the pattern recognition approach. In general, specific geometric entities are assumed to exist as elements of satellite construction. Such items as parabolic antennas, solar cell arrays or mirror/lens arrays are specific examples. Prior to generation of an albedomorphic solution, the presence of such structures might be detected by analysis of the measurement data, treating it as a two-dimensional array (in essence a transform of the object). The brightness contribution of a detected entity could be simulated and subtracted from the measured signal. Anomalies in the detected vs. measured signals might provide useful information with respect to the interference problems.

The usefulness of pattern recognition in this context is, at present, hypothetical. However, the success of the specular reflector study provides some support for the concepts usefulness.

3. The Data Base

The preceding section has dealt with the creation of an abstraction, a mathematical/computational model of the orbiting satellite surface geometry problem. Given the existence of such a model and the mathematical/computational tools for implementing a solution, there remains the problem of specifying the form and nature of the brightness measurements. As will be seen in the description below, this real world data differs from ideal in many respects. The measurement data suffers from: (1) noise inherent in the measurement technology; (2) absent readings of varying length; (3) anomalies due to obscuration of the satellite and/or introduction of (apparently) local brightness.

A second data input is the a priori information which describes orbital position and orientation information. This data was supplied by the research sponsor for the given data types. The data was supplied for only a limited set of parameters (in particular for the $\theta_{\Sigma}(t)$ which corresponded to the perpendicular bisector of the angle g). It is clear that other necessary data can be computed and/or supplied.

The last data necessary for verification of the research results in a specification of the surface geometry and albedo data of the satellite or satellites measured on the input data tapes. This data was not available. As will be described later, development of physical and/or mathematical phantoms can be used to alleviate the problem when such measurements have not been made of satellites prior to launch.

3.1 Mode of collection

The following summarizes discussions with personnel of the sponsoring agency. It is as complete a description of the data collection process as is available.

On-site instrumentation is a telescope equipped with a photo-multiplier for light intensity measurement and an analog instrumentation recorder for data storage. Equipment appears to be operated under the control of on-site personnel. The field-of-view of the instrument encompasses a region of the sky somewhat larger in angular measure than the satellite itself. Calibration of the system is indeterminate.

Data, in the form of analog tapes, is sent to a central site. The data is sampled at a fixed rate (100 Hertz) and converted to digital form. The operation of the on-site instrument creates data sequences corresponding to continuous periods of operation. Conversion to digital form requires some concession to the limits of the hardware in the system used for the conversion (a PDP-11). In particular, no data segment may exist which is larger than 32768 measurements. No physical tape record may exist which is longer than 4096 words. As a result, a data segment may be recorded in one or more segments, each consisting of one or more physical tape records of varying length. Each segment is headed by a record denoting the number of measurements present in the segment.

On the tape, each 16-bit measurement represents 100 times the stellar magnitude measured by the instrument. Some

processing to convert for range factors has been included in the conversion.

3.2 Clean and dirty data

As noted previously, the data recorded is "real-world" data. It is captured at sites at which control of the measurement environment is impossible. The data thus varies considerably from the ideal results that a simulation would yield.

Since the data collection instrument is under human control, it is operated for varying lengths of time. In any one sample tape, gaps exist between sequences of measurements. No data is available in these gaps. Even if the instruments were to be run continuously, reduced visibility due to atmospheric conditions would effectively create such gaps.

The data which is present on the tapes is far from ideal. Since the field-of-view of the instrument is larger than the satellite, background sky glow contributes to the measured brightness. In several cases, the satellite passes close to star positions and thus the combined brightness of a star and the satellite is measured. Atmospheric effects including turbulence, cloud cover and, possibly, precipitation interfere with light transmission, yielding less intense or lower contrast measurements. Lastly, a substantial number of artifacts present in the data appear to be the results of local interference. In particular, it is common for the first 8-10 seconds of a sequence to be measured as a continuous, extremely

bright streak. An educated guess is that a light source local to the instrument (work-light) is left on until the operator has confirmed that the instrument is operational. Another local effect seems to be an occasional dark period which might be attributed to local obscuration of the sky.

Ideal data for a complex geometry could be expected to yield a complex waveform. The measured data contains this complex waveform with substantial artifacts and noise added. The artifacts include: omission of data due to operational requirements, atmospheric effects and local interference; false data due to local or astronomical light sources; and, random (or pseudo-random) noise due to atmospheric and sky-light effects. To these effects are added the instrumental artifacts of optical effects, roundoff error and measurement range limitations. The measured data appears to be quite noisy.

It is important to state that these problems are intrinsic to the collection of data outside of controlled laboratory environments. Additionally, the data was gathered prior to any possible knowledge of the nature of this research project. No portion of this document is to be interpreted as implicitly or explicitly critical of any agency or individual.

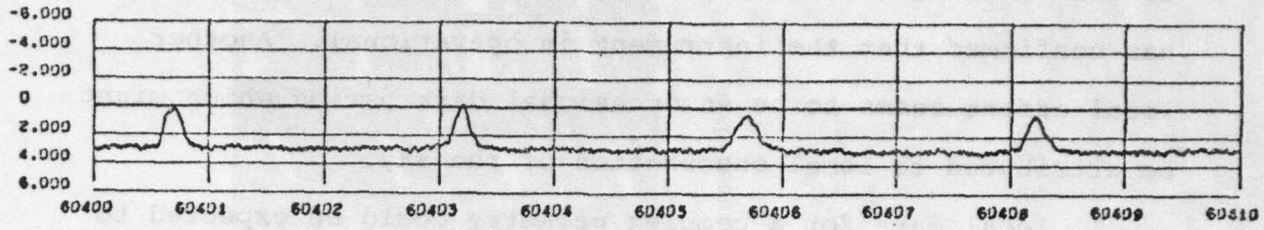

Normal single-peak data, minimal noise

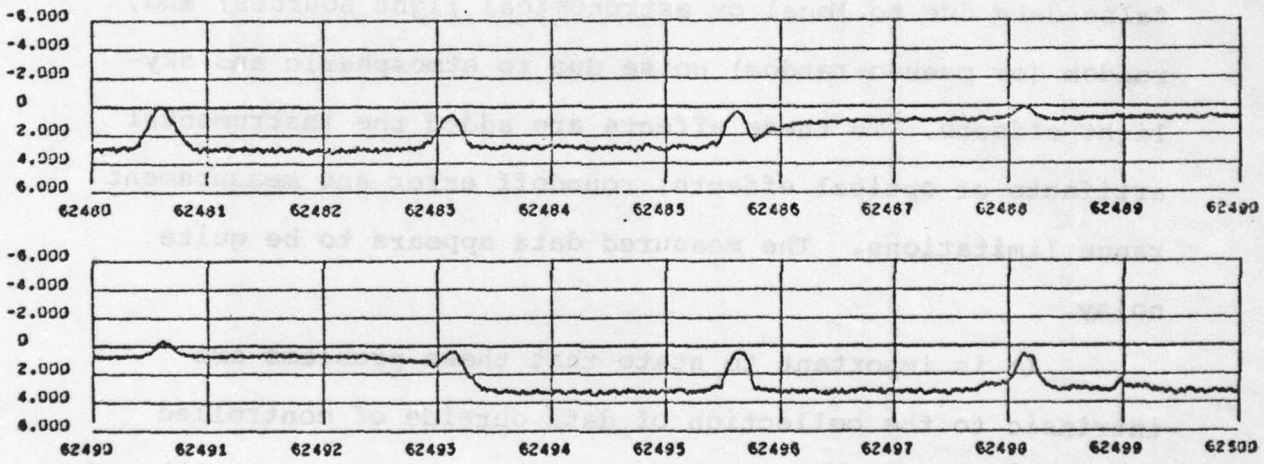

Normal single-peak data, minimal noise, background star from 62486-62493

Figure 3.1: Examples of plotted photometric data. Vertical scale is in stellar magnitude, horizontal scale is time of day in seconds. Sampling rate is 100 hertz.

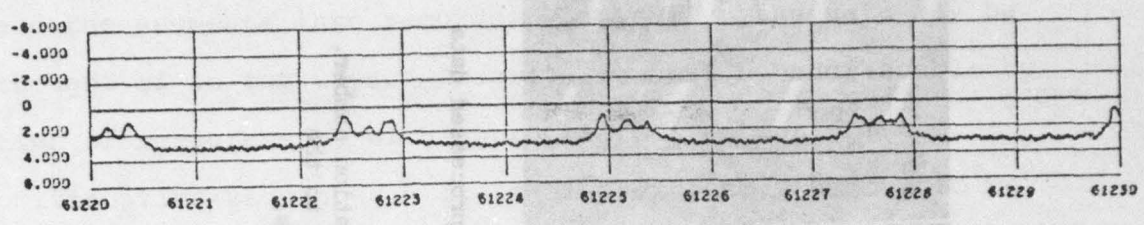

Normal multiple-peak data, minimal noise

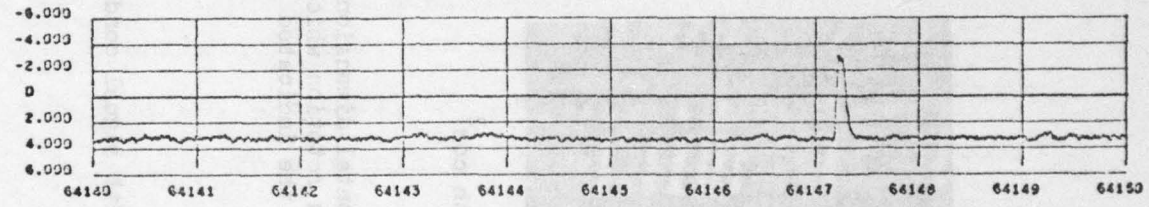

Low amplitude data with single strong peak. Note weak peak at 64143.8.

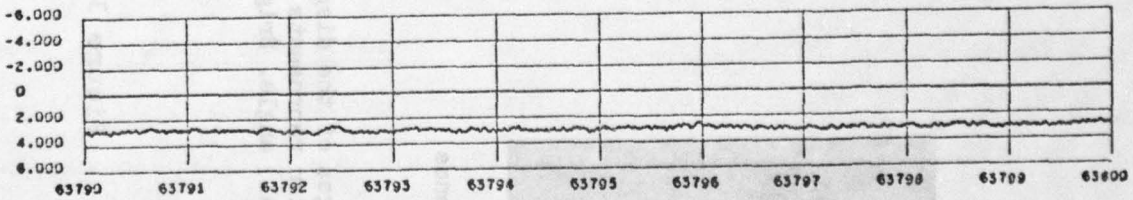

Low amplitude data. Note weak peaks at 63792.4,63794.2,63796.0 .

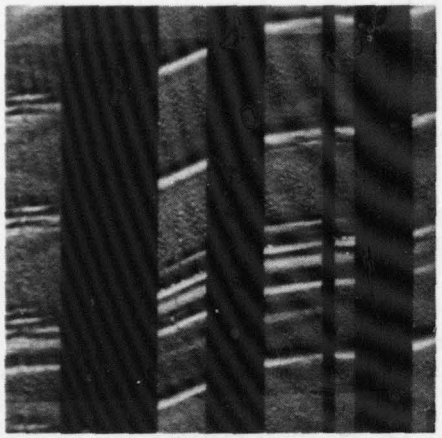

First forward difference

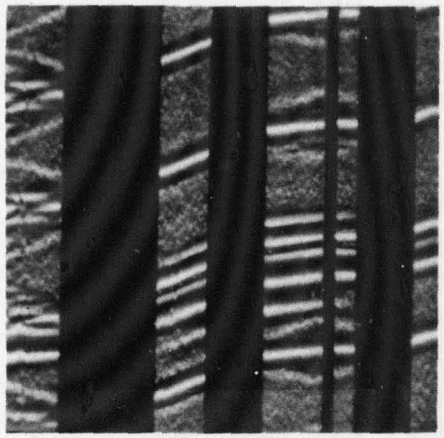

Correlation with $\cos^2$

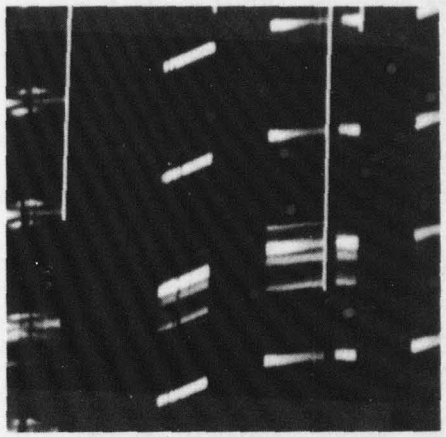

Unprocessed data

Full screen images of the displayed data. Horizontal dimension represents rotation number. Vertical dimension represents time offset within rotation which is equivalent to the rotational (axial) angle. Brightness represents the indicated function's value.

Figure 3.2: Input data with signal conditioning

3.3 Data management

A single tape contains up to 10^6 16-bit light intensity measurements. The tape is broken up physically into segments and the segments into records. Logically, the data may be thought of in two ways. Clearly, it must be addressable by time of measurement, with appropriate treatment of the omitted time sequences. It is also extremely useful to be able to address the data in relation to the local rotations which it undergoes. Specifically, a two-dimensional system of rotation number and time (angle) offset within that rotation are a useful, if not necessary, scheme of reference.

While no effort was made to do so in the initial study, it would clearly be useful to coordinate data gathered with respect to a satellite at different times. This would allow for noise effect reduction and completion of missing or obscured data. The on-line maintenance of several million words of data would require use of an appropriately designed data base management sub-system.

3.4 Phantom generation

It is, of course, desirable to measure the correctness of the results of any computation. Since precise measurements of the geometry and albedo of the observed satellites were not made prior to launch, it is not possible to verify any results. Since the satellites and the data used pre-date this study, no reason existed for such measurements to have been made. The experiences of the Medical Image Processing Group of the Department of Computer Science at SUNY Buffalo suggest

a useful approach to algorithm verification. (11, 12)

A phantom is a model of an object whose precise properties are known. Measurements taken using the phantom may be processed and the results compared with the phantom. For the sake of economy and convenience, a mathematically defined phantom, designed using an interactive computer system, provides a powerful tool for verification of algorithms.

The phantom, along with a program to simulate the physical phenomenon involved (including noise perhaps), would be used to generate appropriate input data to the algorithm being tested. Results could be verified with the original model.

An alternative to the mathematical phantom is the use of scale models and local measurement. A small laboratory apparatus could then be used to make measurements similar to those provided by actual sites. Again, results would be verifiable.

4. A Special Case: Specular Reflectors

This report is the result of a study initiated by the Rome Air Development Center of the United States Air Force. The problem definition was restricted to designing a system to detect, represent and interactively geometrically edit the specular reflectors on an orbiting earth satellite.

Specular reflectors are characterized in the data by sharp peaks. These peaks are due to the directionality of the reflecting surface. As noted earlier, the specular reflector is characterized by a $\cos^n$ law. The higher the power of n, the more specular or mirror-like the reflector.

4.1 Specular peaks and ridges

Consider the illuminator/reflector/observer system of Figure 4.1. The illuminator may be considered a point source. Two related coordinate systems are useful in describing the satellite's geometry. The static (Σ)coordinate system has as its reference coordinates the axis of rotation of the satellite, the geometric axis; and, a normal to the first axis which points north, i.e. towards the Earth's polar axis. These two axes are used as references for ϕ_ε and θ_ε. The second coordinate system (σ) may be thought of as rigidly attached to the rotating satellite. Its first reference also coincides with the axis of rotation of the satellite. The second axis rotates with the satellite and is defined by the rotational position of the satellite within its period of rotation. These coordinates are denoted by θ_σ and ϕ_σ. The relation between the Σ and σ system, for a satellite rotating at a rate v is:

$$\theta_\sigma = 2\pi\, vt + \theta_\Sigma \qquad (9)$$

For a specular reflector, this yields a brightness function of

$$B(t) = a(\cos(2\pi\, vt + {}_i\theta_\sigma)\, \cos(2\pi\, vt + {}_e\theta_\sigma))^n \qquad (10)$$

(from the previously defined brightness function with w=1). This function is a maximum where $|{}_i\theta_\sigma| = |{}_e\theta_\sigma|$, i.e. when the angle of incidence equals the angle of reflection.

One may think of such a reflector as a revolving mirror, scanning its environment. The angle of environment viewed varies with the instantaneous value of ${}_e\theta_\sigma$. The maximum value of the viewing angle occurs when ${}_e\theta_\sigma = 0$. Consider, for instance, a 200 meter reflector at a distance of 10000 km. The viewed angle is $2 \tan^{-1}(10^{-5}) \cong 0^\circ\ 0'\ 2''$. The existence of a 200 m. pure specular reflector is unlikely, but it serves to illustrate the extremely narrow scan angles subtended by specular reflectors.

The illuminator in the earth satellite problem is not a point source. The sun represents a disk of angular diameter of approximately 8×10^{-3} radians or $.5^\circ$. We are dealing now with a three-dimensional system in which ${}_i\theta_\Sigma$ and ${}_e\phi_\Sigma$ vary slowly (as, of course, do ${}_i\phi_\sigma$ and ${}_e\phi_\sigma$) while ${}_i\theta_\sigma$ and ${}_e\theta_\sigma$ vary with a rate related to the rotational velocity of the satellite (approximately six revolutions per minute, with a period of approximately ten seconds). The effect of these two disparate rates is seen in a two-dimensional display of the brightness of data (Fig. 4.2) in which the

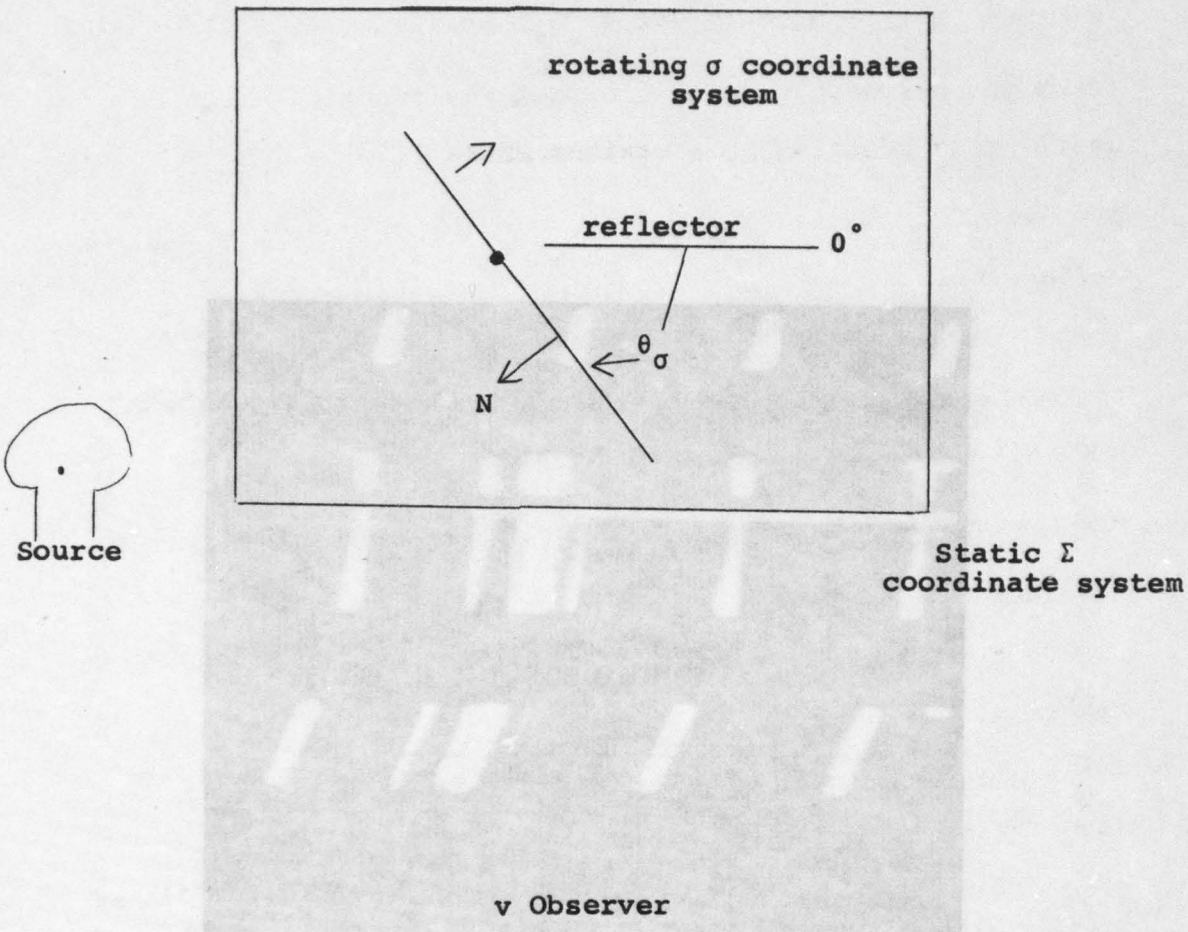

Fig. 4.1 Illuminator, reflector, and observer system

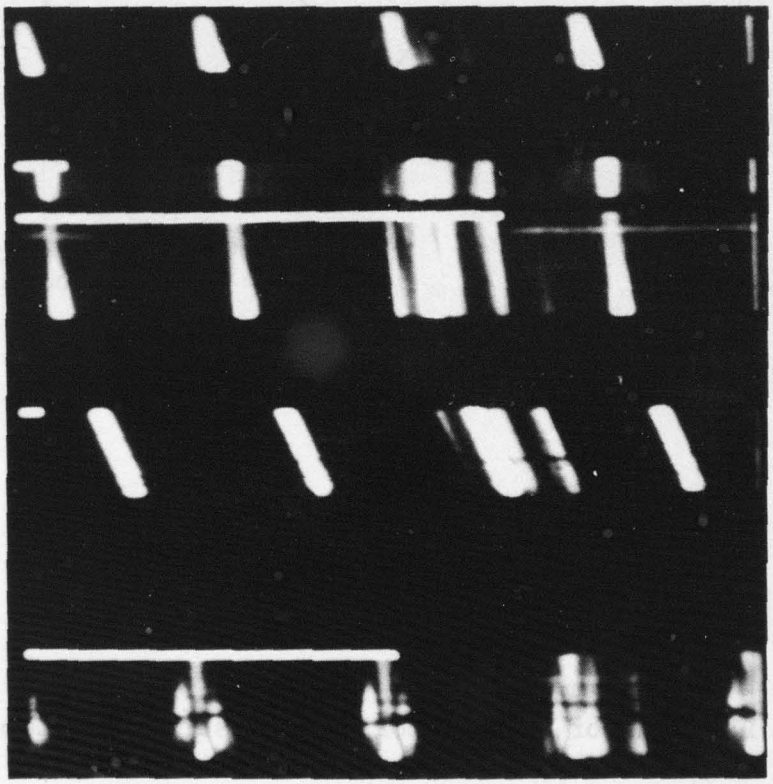

Fig. 4.2a Display of brightness data. Horizontal offset is time offset within rotation; consecutive rotations from top to bottom. Note gaps in data, multiple peaks,noise.

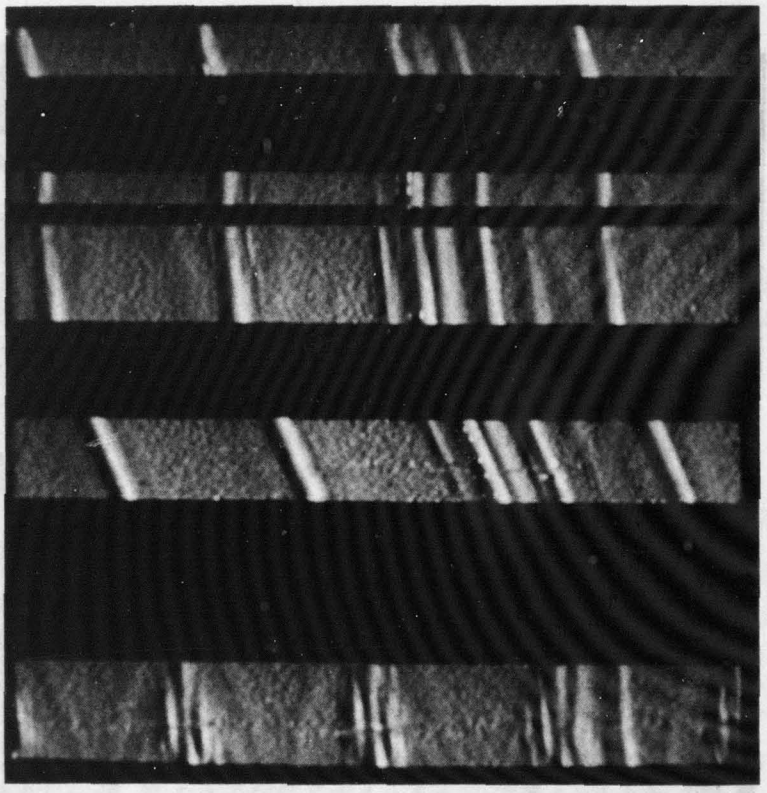

Fig. 4.2b **Display of first** forward **difference data. Data appears as surface side-lit from right. Emphasizes noise and helps seperate multiple peaks.**

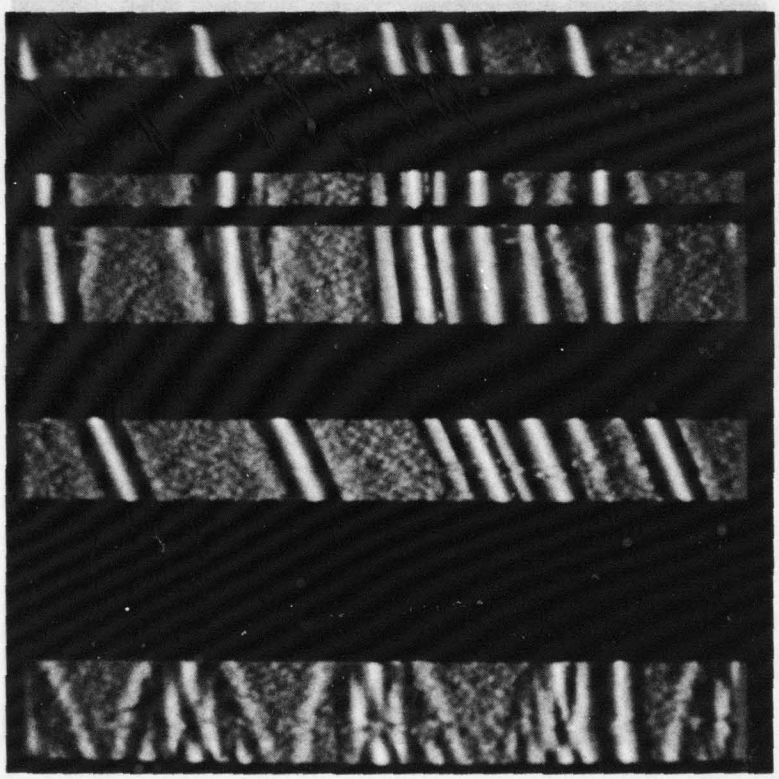

Fig. 4.2c Display of correlation data. Note black(negative) areas on both sides of ridges. Comparison with previous two figures will point out the emphasis of weak peaks and speration of multiple peaks.

vertical dimension represents rotation number and the horizontal dimension represents time offset within each rotation.

For each rotation, θ_Σ may be assumed constant. When the three-dimensional scan prism defined by the planar reflector with the observation point scans an unilluminated portion of the sky, no contribution of the polygon is present in the brightness. As the satellite rotates, the scan pyramid sweeps out a narrow, almost planar segment of space. As θ slowly varies, consecutive, adjacent "pseudo-planes" are swept. When such a pseudo plane intersects the disk of the sun, a peak is detected in the brightness data. Each successive rotation scans an adjacent chordal piece of the sun. This leads to a succession of peaks whose width and height vary with successive chordal regions of the disk. Such a succession of peaks, occurring in the data of consecutive rotations at approximately the same offset within each rotation, will be called a ridge. The maximum peak of each ridge will occur when

$$\min \left\{ \begin{matrix} |{}_i\theta_\sigma| & |{}_e\theta_\sigma| \\ |{}_i\phi_\sigma| & |{}_e\theta_\sigma| \end{matrix} \right\} \text{ occurs within the rotation}$$

The maximum value of a ridge corresponds to the same expression within the ridge. The detection of a ridge maximum thus defines the orientation of the surface normal of

the reflector. The actual value of the ridge maximum is related to the polygon area.

The technique for determining the existence, orientation and area of a specular reflector is to detect a peak, follow its ridge (ridge run) and detect and analyze the ridge maximum.

4.2 Peak finding

Two classes of algorithms are necessary in this stage of processing: peak-detection and ridge running. These processes must be considered in the context of noisy and incomplete data. A number of approaches were examined in each case.

Peak-detector I: Fixed-limits, minimum width. (PROCEDURE PD1)

Algorithm I uses a fixed minimum value (threshhold) to scan the data. When the data exceeds this limit for at least a minimum number of samples, a peak is detected. Procedure PD1 illustrates the technique. While it is simple and efficient, the algorithm suffers from a number of shortcomings. It detects peaks based on values rather than slope or shape. An upward or downward drift in the data will cause false peak detection or missed peaks respectively. Multiple overlapping peaks will not be separated, but will be detected as a single wide peak. The effect of noise will be to somewhat narrow peaks, as any value below the minimum value terminates a peak.

Peak-detector II: First Difference, minimum positive slope, alternating order (Procedure PDP2)

```
Procedure PD1(INPUT,OUTPUT);

CONST   LENGTH=n;
VAR     MINVALUE,MINWIDTH:INTEGER;
        DATA:ARRAY(1..LENGTH) OF INTEGER;
        J,PEAK          :INTEGER;
BEGIN
        COUNT:=0;
        FOR   J=1 TO LENGTH DO
           BEGIN
              IF(DATA(J)>=MINVALUE
                THEN    COUNT:=COUNT+1
                ELSE    BEGIN
                          IF   COUNT>=MINWIDTH
                             THEN   WRITE("PEAK AT", J-COUNT/2);
                          COUNT:=0
                        END
           END;
END
```

Peak-detector II: Minimum positive slope, alternating order (PROCEDURE PD2)

```
Procedure PD2(INPUT,OUTPUT);

   COST     LENGTH=n;
            PREV SLOPE,
   VAR      MINSLOPE:INTEGER
            DATA:ARRAY(1..LENGTH)OF INTEGER;
            PEAK:ARRAY(1..LENGTH)OF BOOLEAN;
            J, SLOPE:INTEGER; FOUND:BOOLEAN
   BEGIN
            PREVSLOPE:=0; FOUND:=FALSE
            MINSLOPE:=Ø;
            FOR J:=1 TO LENGTH DO PEAK[J]:=FALSE;
            FOR J:=2 TO LENGTH DO
              BEGIN SLOPE:=DATA[J]-DATA[J-1]
                    IF (SLOPE>=MINSLOPE)FOUND:=TRUE;
                    IF ((SLOPE<Ø)∧(PREVSLOPE>=Ø)∧FOUND
                       THEN PEAK[J]:=TRUE;
                    PREVSLOPE:=SLOPE
              END;

            FOR  J=LENGTH-1 TO 1 BY -1 DO
              BEGIN
                    SLOPE:=DATA[j]-DATA[J+1];
                    IF(SLOPE>=MINSLOPE)THEN FOUND:=TRUE;
                    IF((SLOPE<0)∧(PREVSLOPE>=0)∧FOUND)
                      THEN PEAK[J]=TRUE;
                    PREVSLOPE:=SLOPE
              END;
            WRITE(PEAK);
END.
```

Procedure PD2 illustrates a second technique. The data is scanned first in one direction, then in the other. A semi-peak is recorded if the slope in the direction of scan achieves some minimum positive value and then becomes zero or negative. When two semi-peaks are sufficiently close, a peak is denoted at their bisection. The use of a minimum slope requirement prevents drift effects. The use of minimum semi-peak intervals avoids detection of plateaus. This method is essentially an analysis of the first derivatives as approximated by first differences for passage through zero. The minimum slope requirements allow for only positive peaks. As a technique using the first derivative, this approach tends to emphasize noise. Indeed, this algorithm will detect as up to 20% of the data points as peaks in sufficiently noisy data. The scheme is extremely effective in "clean" data.

Algorithm PD2 may be less noise sensitive by redefining the slope computation. For example, the slope might be that of a regression line approximating some collection of n consecutive points. Alternatively, one might average values to eliminate noise effects. This might be done "horizontally" by summing consecutive values of "vertically" by summing consecutive rotation values when $d\theta/dt$ is small. Instead of redefining the slope, it is also feasible to place a minimum-run-length requirement on the number of slope values exceeding MINSLOPE.

Peak-detector III: Shape detection by convolution/correlation

Consider n consecutive values of the data to be an

n-vector. This n-vector will now be transformed by subtracting its mean value from each of its elements. This is a translation of coordinates. A unit vector in n-space is now calculated from the translated n-vector by division of each element by the magnitude of the vector. Note that this normalization process creates a vector which is the mapping of all such n-element sequences of data which vary by a fixed difference or by a constant multiplicative factor. That is:

$$\bar{V} = a\bar{u} + \bar{K} \tag{11}$$

where a is any positive scalar

$\bar{u}$ is the normalized unit vector (canonical shape vector)

$\bar{K}$ is an n-element vector in which all elements are equal to the mean of the elements of $\bar{V}$.

In the case of this data, $\bar{u}$ will be considered a canonical shape vector. Now, define $\bar{w}$ as the n-element canonical shape vector for the pattern whose detection is sought, e.g. $\cos^2(\tau)$. The degree of similarity between two such vectors will be determined by the calculation of

$$S = \bar{u} \cdot \bar{w} \tag{12}$$

This is the correlation coefficient between two sets of data. It represents the cosine of the angle between the two vectors ($\bar{u}$ and $\bar{w}$) which are unit vectors. Since the "shape" defined by the normalization operation is scale and base value independent, this technique is

considered to be a shape detector as opposed to a value or slope detector. The procedure takes successive n-element data sequences, normalizes them and performs the inner-product. If the conversion of each data sequence to canonical shape form were not performed, the process would be equivalent to the convolution of a response function (again, e.g. $\cos^2(\tau)$) with a signal.

The technique tends to be relatively noise-insensitive due to the effects of summation in the inner-product. For a fixed magnitude noise component unrelated to signal magnitude, the effects of noise are greater in small peaks than in large peaks. Multiple peaks are especially well handled since the valleys between the multiple peaks yield very negative correlation values. A simple algorithm such as a minimum value (.6-.8) minimum width peak detector operating on the correlation data works extremely well. Actual data values at the peaks must, of course, come from the data rather than the correlation values.

4.3 Ridge-running

The detection of a single peak in a single rotation is a necessary condition for a specular reflector, but not sufficient. Due to the solar disk chordal scanning phenomenon described earlier, any specular reflector will generate a sequence of peaks, each in a consecutive satellite rotation. Each peak will occur at approximately the same time offset within the rotation. Variations from this fixed offset may be

attributed to error in the rotation time, noise effects on the exact peak location and attitude corrections from the satellite's guidance system.

Once an initial peak has been detected, it is necessary to track the succeeding peaks in the specular "ridge", determine the maximum peak value and time, generate summary data on the ridge, and, upon detection of the end of the ridge, report the specular reflector's existence. This process has been referred to as "ridge-running".

In addition to the functions described above for the ridge-runner, one additional function is necessary. After the data relating to all previously encountered non-terminated ridges has been processed, it is necessary to continue the processing of the peak detector to find any new ridges that have not been previously encountered. The ridge runner must, therefore, tag the data associated with the ridges it processes so that the peaks will not be detected as new peaks.

In the design of the ridge-running algorithm, just as in the design of the peak detection algorithm, it is necessary to take into account the nature of the actual data which has been acquired. As intuition might indicate, the difficulties associated with tracking "large" objects such as peaks are those of omitted or obscured data rather than instantaneous noise. When these phenomena exist for only a few rotations, the problem is solved by allowing in the algorithm for an acceptable number of skipped peaks before forcing termination of the ridge. When larger time intervals of omitted data

exist, the resolution of the problem is more difficult. If the ridge is extremely strong, its structure may be picked up after the omission interval. If this is not the case, the peak terminates at the beginning of the data gap. Particular difficulties arise if the maximum peak occurs in the interval.

Two approaches to ridge-running were investigated during program development. In the early stages of the investigation, an approach which kept full data segments in memory was implemented. This approach was abandoned and the current approach, requiring only a single segment in memory at a time, was implemented.

The segment-wise approach was abandoned for several reasons:

(1) it required at least 32K words for segment storage plus additional memory for program and working memory;

(2) contrary to initial assumptions, many ridges were longer than one segment in length; and

(3) program control flow grew too complex as a result of the pseudo-backtracking requirements of the segment-wise approach.

The segment-wise ridge-runner first read in a segment (not sequence) of data. Its outer loop then began searching for peaks. When a peak was encountered, its ridge was run and tagged to termination. The algorithm then jumps back to the peak detector which continues its search past the initial peak of the ridge just processed. The peak detector thus scans the entire segment. If a ridge completes in a segment, it is reported, otherwise it is "scheduled" for continuation

in the next segment.

The rotation-wise ridge runner operates on a single rotation's data at a time. In those cases where, due to omissions, a portion of a rotation has no data, the missing values are set to a null value. After the rotation data is read, two processes are applied. First, the ridge-runner, which keeps a list of the previously encountered, non-terminated ridges examines the data for each ridge's continuation. Where continuation conditions are met, the ridge description is updated. The peaks associated with continuing ridges are tagged so as not to be confused with new peaks. Terminated ridges are reported and their ridge descriptors deleted from the data structure. The peak detector now analyzes the data to determine if any new peaks are present. If so, ridge descriptors are created for the new ridges.

Since the data for a rotation in fact is circular in the sense that the satellite is rotating, and since the change in θ is so small between successive notations, peaks that occur on rotation boundaries present only a minor problem. The data is addressed modulo the rotation period and the end points in the data are "joined" so that the endpoint peaks are part of a circular list.

4.4 Specular detection subsystem

The process of detecting, analyzing and reporting the existence of specular reflectors from brightness data is performed by the specular detection subsystem (this was referred to in, some earlier communications as the signal

processing phase). Data is provided on digital tape, and the program allows for interactive viewing of the data, inputting of detection parameters and on-line recording of the results. The current version is implemented in FORTRAN on a Data General Eclipse S/200, using a COMTAL color-raster display.

After prompting the user to provide initial parameters, the program provides for viewing the raw data, first forward difference data and the correlation data under user control. Peaks detected as well as peak widths as determined by minimum peak value may also be displayed in real-time. If the input parameters chosen yield inadequate results, the program may, of course, be restarted with different user input.

The output of the program, recorded on disk and/or printed, is a list of specular faces, their orientation and area. Details of program operation are specified in Appendix A.

The program in its current form performs peak detection and ridge-running on the correlation data while extracting peak value data from the raw data. The correlation data is sufficiently smoothed and normalized that minimum-value, minimum-width peak detection is used. A rotation-wise ridge-runner allows for implementation in a reasonable amount of memory.

5. Geometric Editor

The output of the specular detection subsystem is a set of partially specified polygons. Specifically, each polygon is specified by its area and the orientation of its normal. The shape and position of each of these polygons in the space local to the satellite is unknown and, in the context of previous discussion, unknowable. In some sense, a portion of the pieces of a three-dimensional jig-saw puzzle have been created and no knowledge of the "picture" contained in the puzzle has been provided.

If it is assumed that a knowledgeable user exists, then an interactive geometric editor would allow that person to assemble the polygons in a fashion suitable to construction of a feasible satellite geometry. Two requirements exist for this system. The system must allow for manipulation of the geometric elements provided by the specular detector within the orientation constraints created by it. The editor must be natural for a user to interact with.

5.1 Orientation-constrained transformations

The results of specular detection are defined by the orientation of their normals and the area of the associated polygons. The normals are defined in terms of the local satellite coordinate system. This form of definition disallows any transformation which modifies the relative angles between the individual polygon normals. The editor will allow for all other elementary transformations.

Fig. 5.1 Editting system-

The following pages of photographs show some of the capabilities of the Constrained Editting System.

Orientation of the object is given by two rotation angles. The first refers to a tilt of the axis of rotation towards the observer; the second indicates rotation about the axis of rotation.

The light source is denoted by a 3 element direction vector. The z-axis is positive in the line of sight so it is necessary to always have a negative z term to avoid back-lighting.

Many of the images contain a wedge shaped artifact resulting from interference between the cameras focal plane shutter and the display refresh. This artifact does not appear in actual viewing.

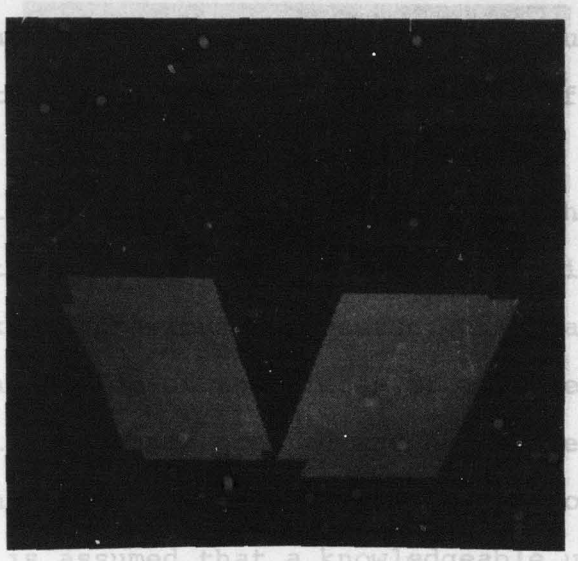

(a) 4 polygons; 0° 0° rotation; flat lighting

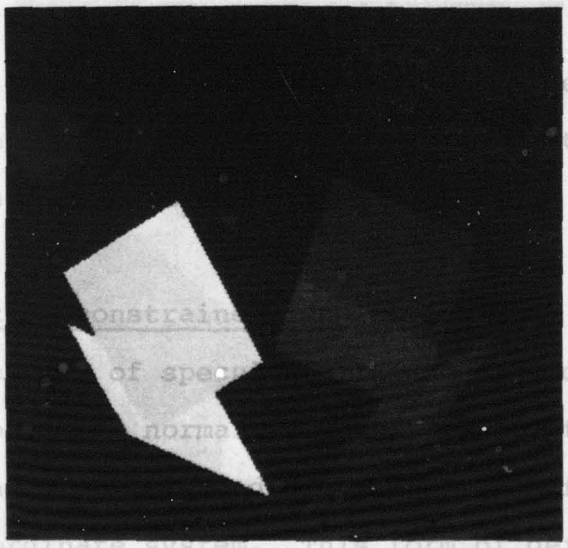

(b) 4 polygons; 0° 30° roation; (-5,0,-1) lighting

Fig. 5.1 Editting system - lighting and orientation change

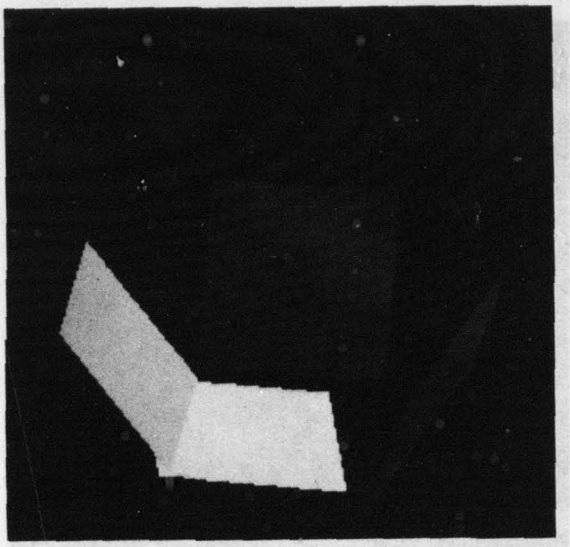

(c) 4 polygons

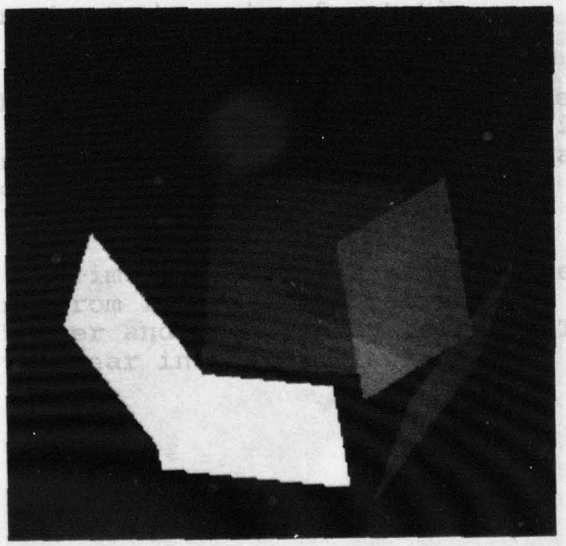

(d) 5 polygons

Fig. 5.1 Editting system-Addition of polygon
30° 30° rotation; (-5,0,-1) lighting

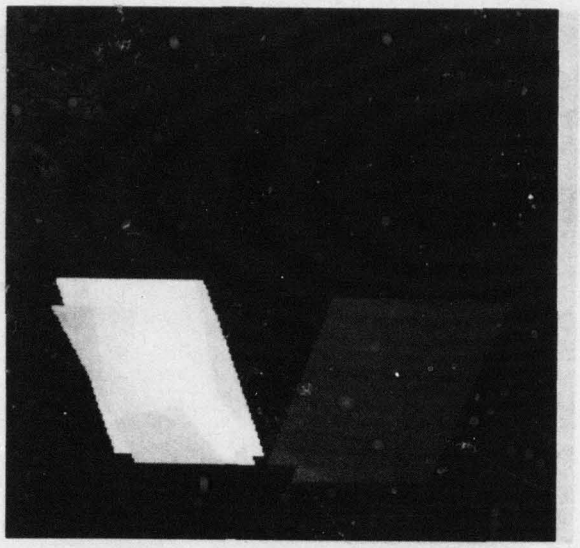

(e) 4 polygons

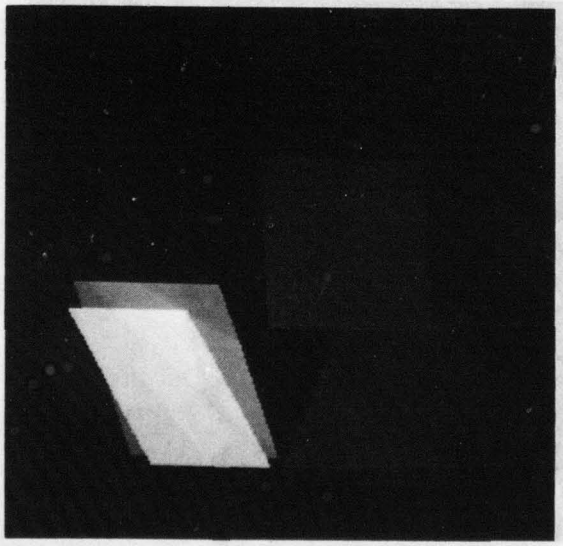

(f) 5 polygons

Fig. 5.1 Editting system- Addition of polygon
0° 0° rotation; (-5,0,-1) lighting

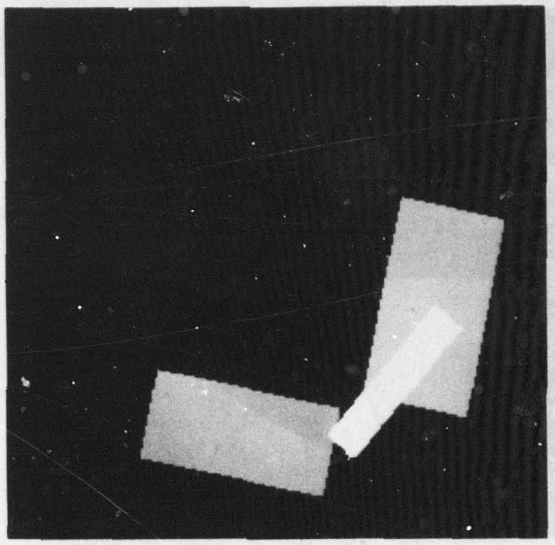

(g) initial view

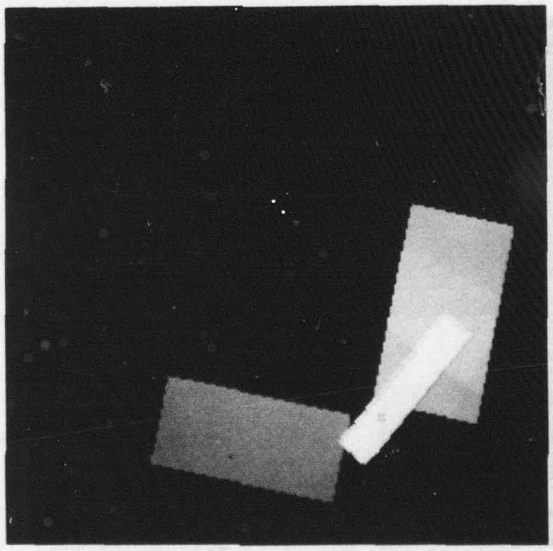

(h) polygon select, note cursor and phantom outline

Fig. 5.1 Editting subsystem- constrained translation
5 polygons; 30° 90° rotation; (-5,0,-1) lighting

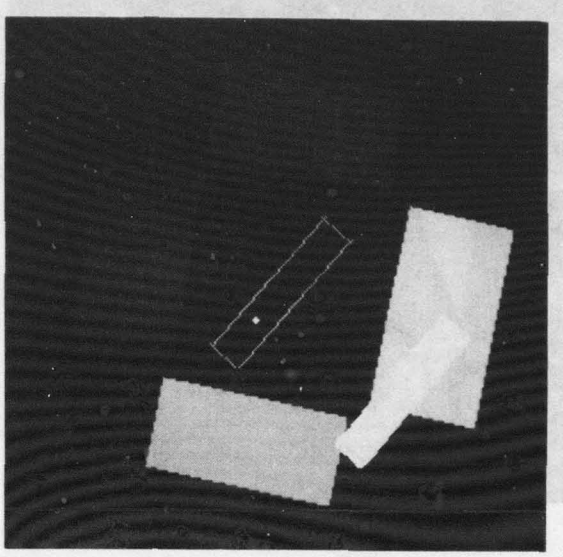

(i) polygon moved parallel to screen; marked by phantom silhouette and controlled by cursor.

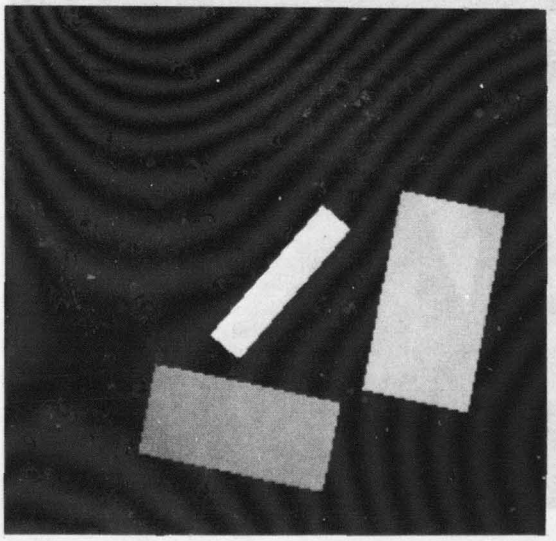

(j) completed translation with actual polygon moved

Fig. 5.1 Editting system- constrained translation (continued)

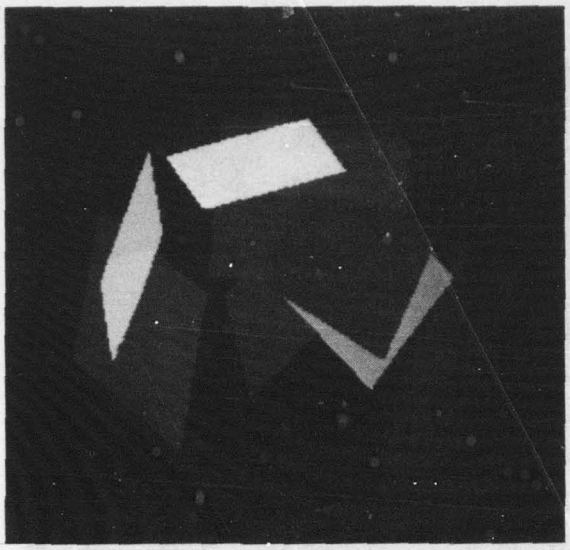

(k) note dark polygon near center of image

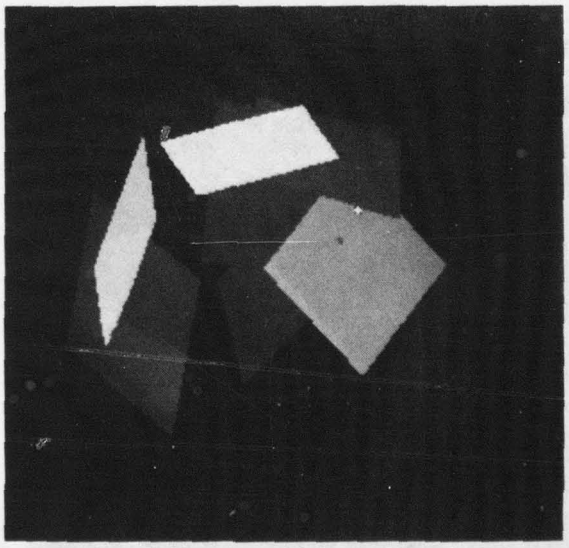

(l) dark central polygon deleted

Fig. 5.1 Editting system- polygon deletion

Translation of whole polygons is clearly required. Rotation of the polygon assembly so as to preserve inter-normal angles is included. This rotation may be defined in terms of the satellite system, e.g. rotation about the central axis, or in terms of the viewers orientation. Heterogeneous scaling of individual polygons will initially be defined as squares of appropriate area. A homogeneous scaling of all polygons about their centroids will allow the user to compensate for scaling effects in the data collection process.

Viewing will be performed in orthographic projection. A z-buffer algorithm will be used for hidden surface removal and shading. Cone of view will be maintained so that no clipping is required.

5.2 Human-computer interface design

An examination of the data provided indicates that at least several score specular reflectors will be detected in a typical sample. The existence of numerous polygons at different orientations will be particularly confusing for a user of the geometric editor. This is particularly severe because of the lack of a priori knowledge of the shape to be generated. The geometric editor provides several aids to assist the user.

An implicit aid, in that it is not under user control, is the use of a shaded image with all hidden surfaces removed as the standard viewing technique. A version of the z-buffer

algorithm is implemented for this. In addition, the user is provided with a set of transformations and viewing orientations to aid his/her perception of the object. Standard views include axial (down the axis of satellite rotation), normal to a selected polygon and equatorial (in a plane normal to the axis of satellite rotation). Arbitrary roll and tilt of the satellite may also be initiated. All polygon translations will be parallel to the viewing plane via track ball control.

A more explicitly realized aid is in the form of polygon management. Polygons will be presented to the user sorted on descending area. Thus, large polygons can be presented and edited to provide an overall framework for placement of the smaller polygons. After a number of polygons have been added, it is necessary to differentiate between those polygons actively being edited and the quiescent polygons providing a background. The active polygons will be referred to as the Polygon Working Set (PWS) in analogy to operating system terminology. Membership in the PWS will be determined on a least recently used basis. While the shading rule will be the same, members of the PWS will appear on the screen in a different color than the background polygons. Typically, PWS size will be limited to ten although the size of the PWS is under user control.

In order to support interrupted editing sessions as well as to allow backtracking in an editing session, a save/restore capability is provided. There is also a hard copy capability from the display screen.

Control of the editor is designed on the Finite State Machine model. Each input acts as a token causing a state transition and action on the transition. States are grouped into classes including:

(1) data base commands;

(2) geometry commands;

and

(3) viewing commands as well as "housekeeping" commands.

The geometric editor has been specifically designed to make use of the principles of effective human-computer communication user specification appears in Appendix B.

5.3 Conclusions of the Specular Geometry Study

Since the original statement of task for this work detailed a study of the feasibility of satellite geometry determination for specular reflectors, it is necessary to state the conclusions reached by this work.

I. The goals of the study have been accomplished. Specular peaks can be identified in the data. Appropriate sequences of peaks, ridges, can be traced, their maximum peak identified and the maximum peaks orientation and area calculated. For the data provided, the best method found is the use of correlation data with a minimum-value, minimum-width peak detector and a rotation-wise ridge follower.

II. The process of interactively editing the output results of specular detection is successfully implemented.

Control of viewing, positioning of polygons and the assembly is achieved in an effective human-computer system. The system has been used successfully to assemble polygon collections and is ready for testing with "knowledgeable" users on real data.

III. While the results achieved are successful in terms of available data, no evaluation of the accuracy of the system is possible without development of a phantom system.

IV. The ability of the system to yield recognizable geometrics of orbiting satellites remains to be demonstrated. The three-dimensional, partially defined jigsaw puzzle that is assembled in the editing phase presents the user with an exceptionally difficult problem. The ability of a human to solve such a puzzle is unproven.

The essence of these conclusions is that the tasks of specular detection and interactive editing are feasible. The effectiveness of these techniques remains to be proven. Specific accomplishments of this study have included:

(a) Development of a mathematical model of the orbiting satellite reflection problem and its associated data acquisition system.

(b) Identification of techniques useful in solving this problem.

(c) Implementation of a specular reflector detection subsystem.

(d) Implementation of an interactive orientation-constrained geometric editor.

6. A Proposal for Solving the Geometry of Orbiting Earth Satellites (GOES)

As the preceding conclusions indicate, the specular study was a success in the sense of accomplishing its goals but did not yield a solution to the more general problem of orbiting satellite surface geometry. The process of analyzing and solving the special specular case has led to a conviction that the more general problem of determining a "good" approximation of the geometry of an orbiting satellite from its recorded brightness is a solvable problem. The approach outlined below is an important result of this study as the description of the specular reflector system.

The approach outlined includes four major subsystems. A data base system is necessary in order to support the large amounts of data associated with the problem. It is also necessary to relate and combine data from different observations of the same satellite. Such an agglomeration of the data will fill in omitted data and/or enable noise reduction in multiply measured data. A phantom-generation system will provide for the definition of well-defined, computationally viable satellite models and the simulation of brightness observations there from. A desirable addition to the computational phantoms would be the availability of a scale-model physical phantom capability. A signal processing/pattern recognition system will provide for the conditioning of input brightness data and for the recognition of a predefined set of

common satellite elements. By use of the simulation capability of the phantom generator, the contribution of the recognized assembly to the brightness could be deleted. Lastly, an albedomorph from projections system would attack the remaining brightness signal to determine an albedomorphic geometry for the remaining portions of the satellite.

This system is different substantially from the specular system in a number of ways:

(1) It attacks the more difficult and important problem of general surface reconstruction of remote objects from reflected brightness, whereas the specular system attacked the special case of specular reflectors:

(2) By including a phantom generation system, the results may be verified as to accuracy;

(3) The system brings to bear a wider variety of tools to attack the more difficult problem. Most specifically, the tools of image reconstruction, pattern recognition and data-base design are added to the graphics and signal processing of the specular study;

(4) The research will begin by extending the mathematical model developed and adapting mathematical solution techniques to the general problem.

6.1 Data-base system

A data-base system for a GOES system must support three

problem-domain classes of data. A priori information relating to satellite orbit, solar position, rotational information etc. is included in the first class. A posteriori data, the resulting satellite geometry, is included in the second class. The third class is the collection of brightness measurements. While the first two classes of data provide no substantial data base problems, the third class is problematical. A typical data tape will contain 10^6 or more brightness measurements. It is reasonable to assume that more than one set of such measurements would be made for a single satellite of interest. It is thus reasonable to expect the data base size for single satellites to exceed 10^7 words in size. In terms of the management and structuring of the data, it is necessary to deal with the problem of overlapping independent measurement parameter ranges in the data. Two possibilities exist when a set of ranges overlap. Data may be used to fill in omitted measurements, in which case the measurement instrument, run-time and environment parameters associated with the data must be properly associated in the data base. In the case of duplicate measurements, it will be left to the signal processing phase to apply appropriate processing for their combination. Thus duplicate data will all be carried with appropriate associations with the data source parameters.

It will be necessary to access data for an individual satellite by absolute time, rotation/offset and, after processing, by ridge number/peak number.

6.2 Phantom Generation

Researchers in the field of computer assisted tomography (CAT) have problems associated with the generation of test data and the verification of processing results. The use of living human subjects provides test data with measurement artifacts from motion, equipment variation, etc. The verification of theprocessing results is impossible unless surgery (or post-mortem) are performed. Even the use of cadavers raises questions of the accuracy of measurement of geometric and/or material properties. A solution to this problem has been the development and use of mathematical phantoms (11, 12).

A mathematical phantom is a mathematically/computationally defined model of a class of objects of interest in terms of the geometry and physical properties along with a means for simulating the physical phenomena under investigation. In the case of CAT the class of objects are two-dimensional slices of anatomical objects and the physical phenomenon is X-ray absorption and physics. In GOES the objects are systems of three-dimensional reflective surfaces* and the physical phenomena are light reflection for various surface materials and finishes.

As noted, availability of a phantom generator allows for creation of well defined experimental objects and simulation

*It may be argued that such surfaces are two degree of freedom mappings of the planar 2-d slices into three-dimensions.

of their behavior. Such a system allows for precise verification of algorithm results. Under field conditions this is, of course, impossible since the satellite is inaccessible and, probably, many of the surface properties are unknown.

A useful adjunct to the mathematical phantom is the use of laboratory phantoms. In the GOES system this could be accomplished by measurement of the geometry, properties and reflective behavior of suitable scale models. Not only would this serve as an additional means for verification of the system, but it would provide a verification for the mathematical phantom.

6.3 Signal Processing/Pattern Recognition

These two aspects of the system require similar computational tools and are thus considered jointly. Signal processing techniques will be used to achieve noise reduction, remove known instrumental artifacts and condition the input signal. Pattern recognition will be used to identify standard satellite surface components by their contribution to the input signal.

From examination of existing satellite structure information, a set of commonly appearing surface geometry components will be determined. Using the phantom generation system, the contribution of such components to brightness will be ascertained. By use of pattern recognition techniques, it is expected that two-dimensional correlation structures will be identified. After identification and

parameter estimation, the contribution of the detected assembly will be simulated and subtracted from the input data.

The use of such techniques as digital filtering, deconvolution and compensation will be applied to improve signal quality. Fourier analysis of the signal will be used as part of the general signal analysis process. At least one of the reconstruction from projections techniques available uses the Discrete Fourier Transform and is thus relevant to signal processing.

6.4 Reconstruction from Projections

As noted earlier, the construction of an albedomorph from brightness data is essentially the reconstruction of a function from a set of its projections. The GOES problem provides a domain for extension of the existing approaches in terms of image domain geometry, noise effects and omitted data problems. The construction of three-dimensional models of orbiting earth satellites which duplicate their reflective behavior as measured is feasible and attainable.

References

1. Phong, B.T., "Illumination for Computer-Generated Images", CACM, Vol. 18, June 1975.

2. Catmull, E., "Computer Display of Curved Surfaces", IEEE Transactions on Computers, June 1975.

3. Gourand, "Continuous Shading of Curved Surfaces", IEEE Transactions on Computers, June 1971.

4. Greenberg, D.P., "An Interdisciplinary Laboratory for Graphics Research and Applications", Computer Graphics, SIGGRAPH, Summer 1977.

5. Horn, "Shape from Shading: A Method for Obtaining the Shape of a Smooth Opaque Object from One View", MAC TR-79, MIT, Cambridge, MA.

6. Herman, G.T., Principles of Reconstruction Algorithms, MIPG-27, Medical Image Processing Group, Department of Computer Science, SUNY/Buffalo.

7. Crowther, R.A., D.J. deRosier and A. Klug, "The Reconstruction of a three-dimensional structure from projections and its application to electron microscroscopy", Proc. Royal Soc. of London, B. 182, 1972, 89-102.

8. Taylor, J.H., "Two-Dimensional Brightness Distributions of Radio Sources from Lunar Occulation Observations", Astrophysical Journal, 1967.

9. Altschuler, M.D. and R.M. Perry, "On Determining the Electron Density of the Solar Corona from K. Cononameter Data, Solar Physics, 1972, Vol. 23.

10. Horn, B.K.P., "Image Intensity Understanding", AIM 335, MIT, Artificial Intelligence Laboratory, August 1975.

11. Simmons, R., Phantom Manual: An Interactive Graphics System for Creation of Test Phantoms, MIPG-13, Medical Image Processing Group, Department of Computer Science, SUNY/Buffalo.

12. Altschuler, M.D., T. Chang and A. Chu, Rapid Computer Generation of Three-Dimensional Phantoms and Their Cone-Beam X-ray Projections, MIPG-16, Medical Image Processing Group, Department of Computer Science, SUNY/Buffalo.

MISSION
of
Rome Air Development Center

RADC plans and executes research, development, test and selected acquisition programs in support of Command, Control Communications and Intelligence (C^3I) activities. Technical and engineering support within areas of technical competence is provided to ESD Program Offices (POs) and other ESD elements. The principal technical mission areas are communications, electromagnetic guidance and control, surveillance of ground and aerospace objects, intelligence data collection and handling, information system technology, ionospheric propagation, solid state sciences, microwave physics and electronic reliability, maintainability and compatibility.

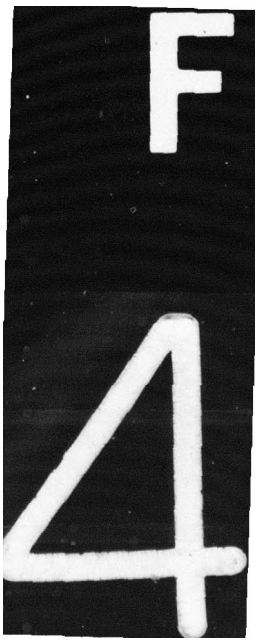
F
4